

August 18, 2004

Thick M-type barium hexaferrite films grown on garnet substrates

C. Vittoria
Northeastern University

S. D. Chen

Recommended Citation

Vittoria, C. and Chen, S. D., "Thick M-type barium hexaferrite films grown on garnet substrates" (2004). *Electrical and Computer Engineering Faculty Publications*. Paper 133. <http://hdl.handle.net/2047/d20002304>

This work is available open access, hosted by Northeastern University.



Thick M-type barium hexaferrite films grown on garnet substrates

S. D. Yoon and C. Vittoria

Citation: *J. Appl. Phys.* **96**, 2131 (2004); doi: 10.1063/1.1769597

View online: <http://dx.doi.org/10.1063/1.1769597>

View Table of Contents: <http://jap.aip.org/resource/1/JAPIAU/v96/i4>

Published by the [American Institute of Physics](#).

Related Articles

Optically driven method for magnetically levitating diamagnetic material using photothermal effect
J. Appl. Phys. **111**, 023909 (2012)

Simultaneous observation of magnetostatic backward volume waves and surface waves in single crystal barium ferrite platelets with in-plane easy axis
J. Appl. Phys. **111**, 023901 (2012)

The effect of Fe²⁺ ions on dielectric and magnetic properties of Yb₃Fe₅O₁₂ ceramics
J. Appl. Phys. **111**, 014112 (2012)

Direct observation of magnetic phase coexistence and magnetization reversal in a Gd_{0.67}Ca_{0.33}MnO₃ thin film
Appl. Phys. Lett. **100**, 022407 (2012)

Epitaxial thin films of p-type spinel ferrite grown by pulsed laser deposition
Appl. Phys. Lett. **99**, 242504 (2011)

Additional information on *J. Appl. Phys.*

Journal Homepage: <http://jap.aip.org/>

Journal Information: http://jap.aip.org/about/about_the_journal

Top downloads: http://jap.aip.org/features/most_downloaded

Information for Authors: <http://jap.aip.org/authors>

ADVERTISEMENT

LakeShore Model 8404 developed with **TOYO Corporation**
NEW AC/DC Hall Effect System Measure mobilities down to 0.001 cm²/V s

Thick M-type barium hexaferrite films grown on garnet substrates

S. D. Yoon and C. Vittoria

Electrical and Computer Engineering Department, Northeastern University, Boston, Massachusetts 02115

(Received 19 December 2003; accepted 19 May 2004)

The deposition and characterization of thick M-type barium hexaferrite ($\text{BaFe}_{12}\text{O}_{19}$) films produced by a modified liquid phase epitaxy deposition technique are reported. The films are deposited on (111) oriented single crystal garnet ($\text{Gd}_3\text{Ga}_5\text{O}_{12}$) substrates. The thickness of the films ranged between 45 and 80 μm with growth rates of up to 40 $\mu\text{m}/\text{h}$. This growth rate is about five times greater than films grown on substrates of (111) magnesium oxide. Although the films are relatively thick, the ferrimagnetic resonance linewidth is remarkably narrow (~ 50 Oe) for external fields applied along the c axis. © 2004 American Institute of Physics. [DOI: 10.1063/1.1769597]

I. INTRODUCTION

High quality, thick barium M-type hexaferrite ($\text{BaFe}_{12}\text{O}_{19}$, BaM) films on various single crystal substrates¹⁻⁴ have been reported. It is important to develop inexpensive technique to grow hexaferrites, if high frequency nonreciprocal microwave devices are to be realized. Previously, we have used (111) magnesium oxide (MgO) single crystal substrates to grow high quality barium M-type hexaferrite films^{1,5} by a modified liquid phase epitaxy (LPE) technique.¹ However, BaM film growth rates on the (111) MgO substrates were limited to 0.05 $\mu\text{m}/\text{min}$ compared with ~ 1 $\mu\text{m}/\text{min}$ reported for yttrium iron garnet ($\text{Y}_3\text{Fe}_5\text{O}_{12}$, YIG) grown on gadolinium gallium garnet (GGG) substrate.^{1,6,7} In order to grow thicker BaM layers on (111) MgO , it required long hours of deposition time. However, longer hours of deposition lead to softening of the MgO substrates.^{3,4} We discovered that the shattering of the MgO substrates occurred when we deposited for about 6 h at 900 °C. Therefore, we needed an alternative substrate for growing thick and high quality BaM films.

The first criterion in our search for an improved substrate material was that the lattice constant mismatch between BaM film and substrate was to be small, on the order of 1%. The next criterion was that thermal expansion mismatch between BaM film and the substrate was also to be small, on the order of 20%. In this paper, we propose to replace MgO with (111) GGG substrates. The mismatch between three unit cells of BaM and (111) GGG is 0.9% with 30% thermal expansion mismatch.^{8,9} Although the thermal expansion mismatch is larger than we had hoped, GGG has high potential as an otherwise suitable material. The hardness of GGG is 9 Moh which is higher than that of MgO (7 Moh). Even though BaM films cracked after 2 h of LPE growth, the total thickness of the resultant BaM films were measured to be 45 and 80 μm for single and double-sided growth, respectively. As evidence of their high crystal quality, the ferrimagnetic resonance (FMR) linewidth was measured to be about 50 Oe. This is a significant in terms of producing thick films of barium hexaferrite.

II. EXPERIMENTAL DETAILS

GGG (111) single crystal substrates were obtained from MTI Corp. The size of the (111) GGG substrate was

$10 \times 10 \times 0.5$ mm³ and the substrates were polished on both front and back sides. All the GGG substrates were cleaned prior to the film growth by using diluted nitric acid solutions and de-ionized (DI) water.

The modified liquid epitaxy deposition technique employed in these studies consists of two procedures. First, a thin layer of barium hexaferrite, i.e., the seed layer, was deposited by pulsed laser ablation deposition (PLD). The thickness of the seed layer was about 0.5 μm . We believe that this is an optimal thickness for the seed layer because delamination of the seed layer was observed for thinner and thicker seed layers during the LPE. Details of seed layers preparation can be found in Refs. 5, 10, and 11.

After the seed layer was prepared, it was rinsed in alcohol and DI water. As the second step in this process, we used a boron-based BaM melt to grow the BaM films by the LPE procedure. Details of the LPE process and boron-based LPE flux melt preparation can be found in Refs. 1, 12, and 13. After 2 h of submersing the seed layer into melt and slowly reducing the melt temperature, the total thickness of the BaM films were measured to be 45 and 80 μm for the single-sided and double-sided growth, respectively.

The thickness measurements were performed using a step profilometer and confirmed by cross section views of scanning electron microscope (SEM) images. Crystallographic properties of the LPE grown BaM/(111) GGG films were determined from $\theta-2\theta$ diffraction measurements using a Rigaku 300 x-ray diffraction (XRD) diffractometer. Vibrating sample magnetometry was performed on all of the BaM films to determine static magnetic properties. Dynamic magnetic and microwave properties were determined by FMR measurements. In the latter, a static magnetic field is applied perpendicular to the film plane, where the c axis of BaM is along the film normal.

III. RESULTS AND DISCUSSION

Growth and microwave magnetic parameters of the thick barium hexaferrite films grown by the modified liquid epitaxy deposition technique are listed in Table I. The BaM films on m -plane sapphire, (1100) Al_2O_3 , substrates had the highest growth rate of the films reported here. However, the c axis of films grown on the m -plane Al_2O_3 crystal was

TABLE I. BaFe₁₂O₁₉ parameters grown by modified LPE technique.

LPE BaM films on substrate	Growth rate ($\mu\text{m/h}$)	FMR linewidth (Oe)	Magnetic easy direction	References
BaM on <i>m</i> -plane (1 $\bar{1}$ 00) Al ₂ O ₃	40–100	80 at 59.9 GHz	Easy direction in the film plane	2–4
BaM on (111) GGG	20–40	40–68 at 58 GHz	Easy direction out of film plane	3 and 4
BaM on (111) MgO	3–5	\sim 27 Oe at 56 GHz	Easy direction out of film plane	1

parallel to the substrate plane. Consequently, we were able to grow BaM films having *c* axis in the film plane as well as perpendicular to the film plane. Readers can refer to more details of BaM films on *m*-plane sapphire substrates reported elsewhere.^{2–4} BaM films grown on (111) GGG and (111) MgO grew with the *c* axis perpendicular to the substrate plane. The crystallographic orientation was obtained from XRD, which is shown in Fig. 1(a) for BaM film on (111) GGG.

The growth rate of the BaM films was found to increase when using (111) GGG substrates (as shown in Table I). Specially, the growth rate increased \sim 20 $\mu\text{m/h}$ when using (111) GGG substrates. The growth rate was as much as five times higher than that measured for growth on (111) MgO substrates.

Figure 1(a) shows a typical XRD spectrum measured from a thick BaM film on (111) GGG. All the diffraction peaks were identified as (001) of BaM peaks by use of ref-

erence data.¹⁴ The peak at $2\theta=45.1^\circ$ is the (111) peak of the GGG substrate. Therefore, the *c* axis of the BaM was along [111] direction of the GGG, which meant that the *c* axis of BaM was out of the film plane. This XRD spectrum also confirmed that the BaM films were pure phase. We also measured the *c*-axis lattice constant of the BaM film to be $23.23\pm 0.03 \text{ \AA}$ from fitting centroids of major (001) peaks. The *c*-axis lattice constant from bulk BaM was reported to be $23.18\pm 0.02 \text{ \AA}$.¹⁵ This indicates that the BaM layer on the (111) GGG plane may be in compression by \sim 0.22%. However, since this value is close to the measurement's uncertainty, we cannot say for certain that the films are indeed compressed. Furthermore, with such thick films we anticipate that the majority of the film is fully relaxed.

We also compared linear thermal expansion coefficient α mismatch between BaM and GGG. The α of BaM was measured to be $10\times 10^{-6}/\text{K}$ by previous researchers,^{16,17} whereas α of GGG is reported to be $2\text{--}5\times 10^{-6}/\text{K}$ for 300–800 K. However, the α for both BaM and GGG are known to be nonlinear functions of temperature above 800 K. The large thermal expansion coefficient mismatch as function of temperature between BaM and GGG induced compressed stress for the LPE BaM films. Eventually the BaM films cracked when cooling from high temperature to room temperature during the LPE process.

The rocking curve for the (008) peak for the 45 μm thick BaM film on (111) GGG substrate is shown in Fig. 1(b). The full width at half maximum (FWHM) of this peak was measured to be $\Delta\theta=0.08^\circ$. This FWHM is \sim 60% smaller than the FWHM measured for the same system on similar substrates grown by PLD (see Ref. 10). The FWHM values are evidence of minimal mosaicity of BaM crystal on (111) GGG substrate.

Figure 2 shows the surface morphology of the 45 μm thick BaM film on the (111) GGG substrate, which were taken from SEM and is typical for other samples. The thickness of the hexagonal plates in the SEM image was 1 μm with smooth surface morphology. The largest hexagonal plate was measured to be \sim 40 μm in diameter. This SEM surface image also confirmed that the *c* axis of the BaM layers was perpendicular to the film plane.

dc magnetic properties were obtained from static magnetization hysteresis loops. Figure 3 shows the hysteresis loops for the as-produced BaM seed layers grown by PLD [Fig. 3(a)] and the as-produced BaM layers after 2 h of LPE growth [Fig. 3(b)]. Since GGG is a known paramagnet at room temperature, original vibrating-sample magnetometer

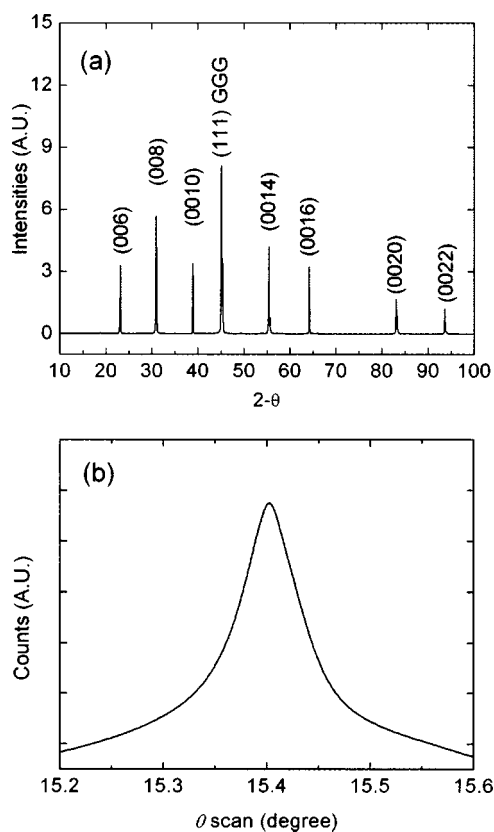


FIG. 1. (a) X-ray diffraction spectrum from a 45 μm thick BaFe₁₂O₁₉ films on (111) Gd₃Ga₅O₁₂ substrate. (b) Rocking curve θ scan of the (008) peak.

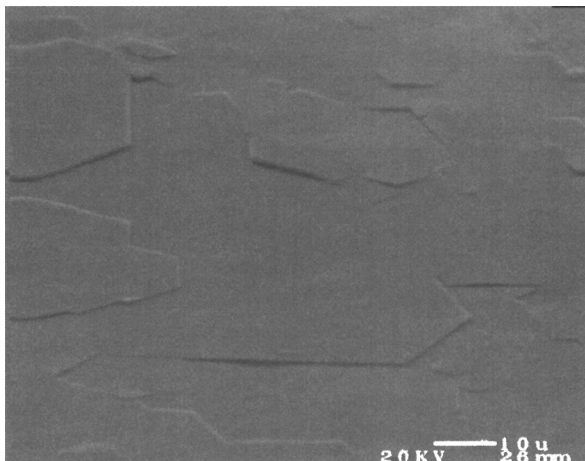


FIG. 2. Surface morphology of the LPE grown $45\ \mu\text{m}$ BaM films on (111) GGG.

(VSM) hysteresis loops data contained paramagnetic and ferromagnetic contributions. The hysteresis loops in Fig. 3 were obtained by subtracting the paramagnetic background of (111) GGG substrate from the total moment. Solid lines in Fig. 3 were collected for the static magnetic field H applied perpendicular to the film plane (out-of-plane). Alternatively, the dashed lines data were taken for the static magnetic field H applied parallel to the film plane (in plane). Since the magnetic easy axis of the BaM film is along the c axis, both

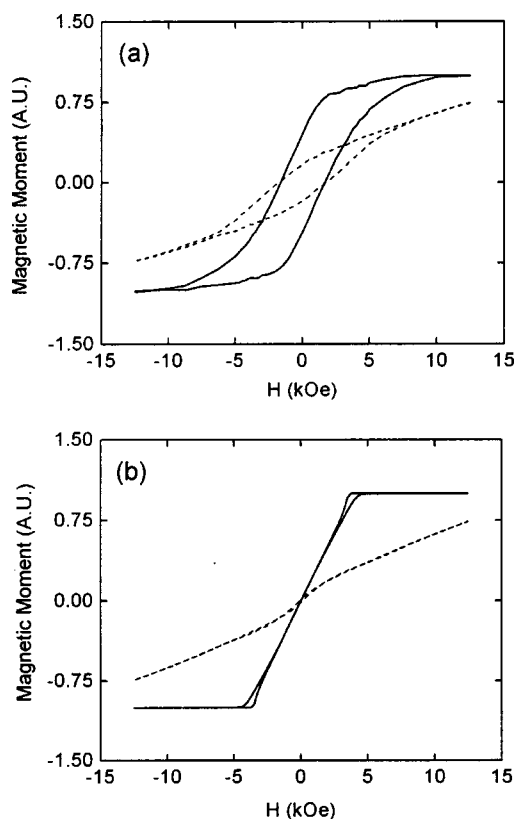


FIG. 3. Magnetic hysteresis loops for BaM on (111) GGG. Solid and dashed lines show dc H field applied parallel and perpendicular to the c axis. (a) VSM hysteresis loops show for $0.5\ \mu\text{m}$ thick seed layers of BaM grown PLD. (b) VSM hysteresis loops for a $45\ \mu\text{m}$ thick BaM layers grown by LPE.

hysteresis loops exhibited strong uniaxial anisotropy. The data in Fig. 3(a) were measured for the seed layer only. Since the easy magnetization axis is perpendicular to the film plane, the BaM films can be easily saturated in the out-of-plane direction. The saturation magnetization ($4\pi M_s$) value for the $45\ \mu\text{m}$ thick films was found to be $4.6 \pm 0.1\ \text{kG}$ at room temperature for the out-of-plane hysteresis loop [Fig. 3(b)]. This value is very close to the bulk values found in the literature,¹⁵ which range from 4.63 to 4.78 kG at room temperature. For in-plane hysteresis loop measurement, the BaM films were not saturated in the 12.5 kOe field due to their large uniaxial anisotropy field H_A . The H_A value for BaM material is reported to be about 17.0 kOe.^{15,18}

From Fig. 3(a), the seed layers exhibit high coercivity H_c in both the out-of-plane and in-plane directions. The value of H_c was measured to be 1.9 kOe. Additionally, remanent magnetization M_r was measured to be $\sim 50\%$ and $\sim 24\%$ of their saturation moment M_s from the out-of-plane and the in-plane hysteresis loops, respectively. However, this high H_c behavior was reduced after 2 h of LPE growth as shown in Fig. 3(b). In this sample, the H_c of in-plane and out-of-plane hysteresis loops were measured to be ~ 0.13 and 0.01 kOe, respectively. The higher H_c observed in the seed layers may be explained in terms of surface morphology and inhomogeneity of the PLD BaM film. However, the high coercivity of the seed layer did not affect the LPE growth of the thick films.

Microwave properties were measured by FMR. In these measurements the applied magnetic field was swept while the frequency was fixed using a TE_{01} mode propagation in a U band (40–60 GHz) waveguide. Since the magnetic easy axis was perpendicular to the film plane, we applied the static magnetic field H perpendicular to the film plane. Consequently, the dynamic magnetic field \vec{h} was applied in the plane of the BaM film. The FMR response was measured at 58 GHz (see Fig. 4). The FMR linewidth ΔH was measured to be 67 Oe which is relatively narrow for such a thick film of BaM.¹⁸ The FMR ΔH of 67–85 Oe was measured in the frequency range of 47–60 GHz, respectively. The distribution of ΔH versus frequency is shown in Fig. 4(c). ΔH peaks near 48 GHz and decreases with increasing frequency. This unusual trend of ΔH with frequency may be attributed to the sample size and the sample position in the waveguide. The sample size was fairly large at $1 \times 5\ \text{mm}^2$ relative to the wavelength ($\sim 5\ \text{mm}$). This size allows magnetostatic modes to be excited, since the rf field is nonuniform over the sample size. As seen from the FMR spectra, the magnetostatic modes overlap with each other and make the measurement of the intrinsic FMR ΔH potentially unreliable. In order to obtain an intrinsic ΔH , the FMR sample sizes should be very small ($\sim 1/2\ \text{mm}$ diameter) for U-band frequency measurement.¹⁸ Our intent here was to measure ΔH for sample size that are to be used in microwave devices. We averaged all of ΔH values measured in Fig. 3(c) and measured $\Delta H \sim 74.6\ \text{Oe}$.

In Fig. 4(b) the resonant frequency f versus applied field H_r for the $45\ \mu\text{m}$ thick BaM film is shown. In Eq. (1) the FMR relationship is given as

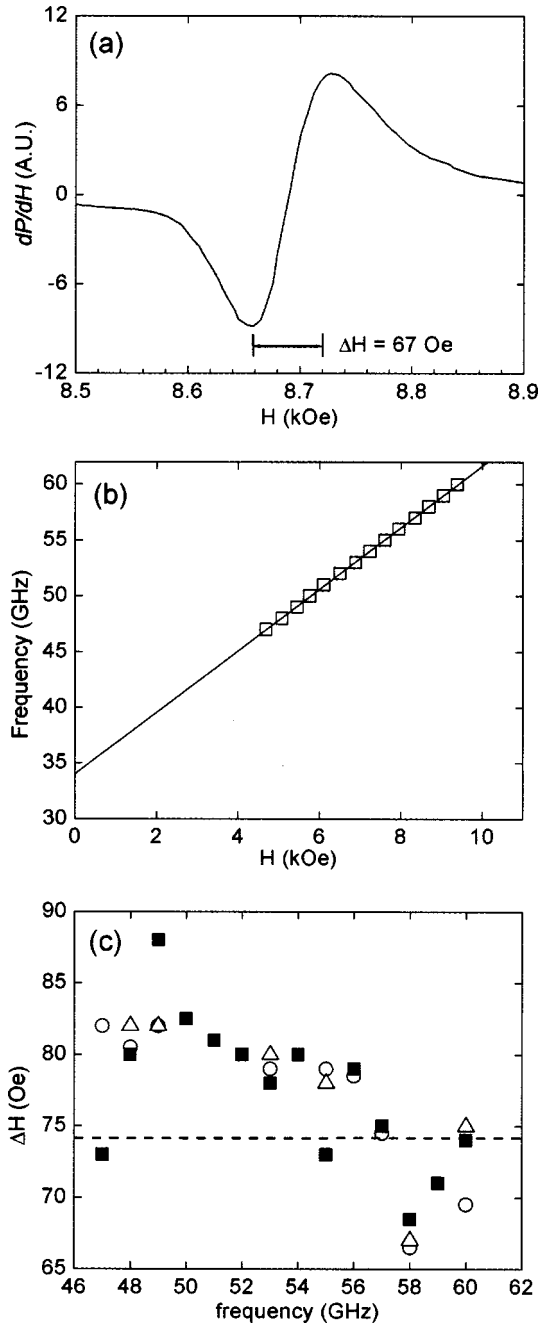


FIG. 4. Ferrimagnetic resonance (FMR) data measured from a 45 μm thick BaM film on a single-sided (111) GGG substrate from 40 to 60 GHz. (a) FMR spectrum for the sample having the narrowest ΔH spectrum measured at 58 GHz. (b) Frequency vs applied magnetic field from 47 to 60 GHz. (c) FMR linewidth vs frequency between 47 and 60 GHz.

$$f = \gamma'(H + H_A - 4\pi M_s), \tag{1}$$

$$\gamma' = \frac{\gamma}{2\pi}, \quad \gamma = g \times 1.4 \times 10^6 \text{ Hz/Oe.}$$

Equation (1) can be derived from the equations of motion and free energy.¹⁹ The g value in Eq. (1), the gyroscopic ratio, is usually about 2.¹⁹ We deduced the g value to be 1.97 ± 0.05 from the linear regression of the f versus H_r data [see Fig. 4(b)]. The value of uniaxial anisotropy field H_A can be deduced by using the relation of frequency versus applied

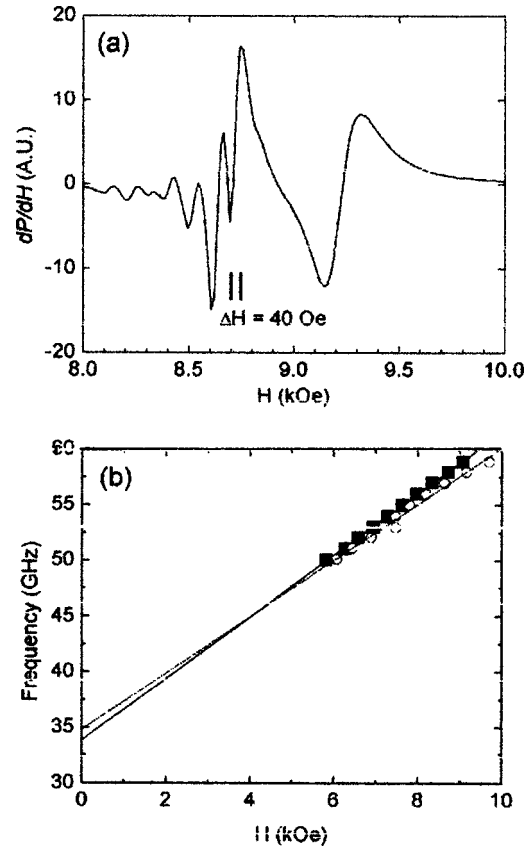


FIG. 5. FMR measurements for BaM films grown on a double-sided (111) GGG substrate by the modified LPE process. (a) FMR spectrum at 58 GHz. (b) Resonant frequency vs H for two FMR modes.

field data shown in Fig. 4(b) and Eq. (1). Since the saturation magnetization field $4\pi M_s$ was obtained to be 4.6 ± 0.1 kG from the hysteresis loops, the uniaxial magnetic anisotropy field $H_A = (f/\gamma')$ reduced to 16.9 ± 0.5 kOe for $H = 4\pi M_s$. The H_A values for BaM single crystal disks or spheres were reported to be 16.2 and 17.3 kOe, respectively, by other researchers.¹⁹

We also have grown BaM films on double-sided (111) GGG substrates. The total film thickness on (111) GGG was measured to be $\sim 80 \mu\text{m}$. Static magnetic hysteresis loops for the double-sided BaM films were nearly identical to the single-sided BaM films. Figure 5 shows typical FMR spectrum measured on an $80 \mu\text{m}$ double-sided BaM film at 58 GHz. The spectrum exhibits many modes, but the main mode can be identified at $H \sim 8.75$ kOe. The FMR ΔH of the film was about 40 Oe. The modes shown below $H \sim 8.75$ appear to be magnetostatic modes. However, the broader absorption mode above the main mode is identified as a surface mode due to inhomogeneity at the boundary between the BaM layers and GGG substrate. The dispersion of the main modes obey the FMR condition of Eq. (1) with $g \sim 1.98$ as deduced from slope of the solid line data shown in Fig. 5(b). However, we have deduced a different g value, ~ 1.80 , from fitting linear regression of dashed line for the broad mode data shown in Fig. 5(b). We attribute the broad line to a FMR surface mode excitation localized at the interface between one surface of the substrate and the magnetic film. The fact that this broad line is observed only when double-sided

growth occurred implies that the two surfaces of the substrate are very different in terms of surface condition. Vittoria and Schelleng²⁰ proposed a model to explain surface mode excitations in garnet films. We believe that this model is appropriate to any ferrite film grown at high temperatures on an inhomogeneous surface and that includes our films.

IV. CONCLUSIONS

Thick, high quality films of BaFe₁₂O₁₉, BaM were prepared on single- and double-sided (111) Gd₃Ga₅O₁₉ substrates by a modified LPE deposition technique. Significant increases in the growth rate of 20 μm/h were obtained. The FMR linewidth was measured to be 40–67 Oe (single sided and double sided) at 58 GHz, which is relatively narrow indicating high quality material for microwave applications. The presence of surface modes on the FMR spectrum was only observed for the double-sided BaM films. This mode may be attributed to interfacial modes between film and substrate at the surface where one surface quality may be inhomogeneous.

ACKNOWLEDGMENTS

This work was supported by Office of Naval Research. The authors thank Vincent Harris for useful comments with respect to the preparation of this manuscript.

- ¹S. G. Wang, S. D. Yoon, and C. Vittoria, *J. Appl. Phys.* **92**, 6728 (2002).
- ²S. D. Yoon and C. Vittoria, *J. Appl. Phys.* **93**, 8597 (2003).
- ³S. D. Yoon and C. Vittoria, *IEEE Trans. Magn.* **39**, 3163 (2003).
- ⁴S. D. Yoon and C. Vittoria, *J. Magn. Mater.* (submitted).
- ⁵S. A. Oliver, S. D. Yoon, I. Kozulin, M. L. Chen, and C. Vittoria, *Appl. Phys. Lett.* **76**, 3612 (2000).
- ⁶R. C. Linares and E. L. Sloan, III, *J. Cryst. Growth* **27**, 249 (1974).
- ⁷R. Hiskes, *J. Cryst. Growth* **27**, 287 (1974).
- ⁸Landolt-Börnstein, *Numerical Data and Functional Relationships in Science and Technology*, edited by K.-H. Hellwege and A. M. Hellwege (Springer, Berlin, 1978), Vol. 12, Part a.
- ⁹V. J. Fratello, H. M. O'Bryan, and C. D. Brandle, *J. Cryst. Growth* **166**, 774 (1996).
- ¹⁰S. R. Shinde, S. E. Lofland, C. S. Ganpule, S. B. Ogale, S. M. Bhagat, T. Venkatesan, and R. Ramesh, *J. Appl. Phys.* **85**, 7459 (1999).
- ¹¹Y.-Y. Song, S. Kalarickal, and C. E. Patton, *J. Appl. Phys.* **94**, 5103 (2003).
- ¹²H. L. Galss and F. S. Stearns, *IEEE Trans. Magn.* **13**, 1241 (1977).
- ¹³H. L. Glass and J. H. W. Liaw, *J. Appl. Phys.* **49**, 1578 (1978).
- ¹⁴International Centre for Diffraction Data (ICDD).
- ¹⁵H. Kojima, in *Ferromagnetic Materials*, edited by E. P. Wohlfarth (North Holland, New York, 1982), Vol. 3.
- ¹⁶P. C. Dorsey, S. B. Qadri, J. L. Feldman, J. S. Horwitz, P. Lubitz, D. B. Chrisey, and J. B. Ings, *J. Appl. Phys.* **79**, 3517 (1996).
- ¹⁷D. Sriam, R. L. Snyder, and V. R. W. Amarakoon, *J. Mater. Res.* **15**, 1349 (2000).
- ¹⁸M. Sparks, *Ferromagnetic-Relaxation Theory* (McGraw-Hill, New York, 1964), pp. 74–104.
- ¹⁹Landolt-Börnstein, *Numerical Data and Functional Relationships in Science and Technology*, edited by K.-H. Hellwege and A. M. Hellwege (Springer, Berlin, 1978), Vol. 4, Part b.
- ²⁰C. Vittoria and J. H. Schelleng, *Phys. Rev. B* **16**, 4020 (1977).